JET–P(91)01

A.C.C. Sips, G.M.D Hogeweij, A.E. Costley, J. O'Rourke,
N.J. Lopes Cardozo, J.C.M de Haas and JET Team

Resolving Apparent Difference between Heat and Density Pulse Propagation in JET and TEXT

Resolving Apparent Difference between Heat and Density Pulse Propagation in JET and TEXT

A.C.C. Sips, G.M.D Hogeweij[1], A.E. Costley, J. O'Rourke,
N.J. Lopes Cardozo[2], J.C.M de Haas[3] and JET Team*

JET-Joint Undertaking, Culham Science Centre, OX14 3DB, Abingdon, UK

[1]*On attachment from the FOM-Instituut voor Plasmafysica, 'Rijnhuizen', Nieuwegein, Netherlands.*
[2]*FOM-Instituut voor Plasmafysica, 'Rijnhuizen', Nieuwegein, Netherlands.*
[3]*Present address: General Atomics, San Diego, California; on attachment from Lawrence Livermore National Laboratories*
** See Appendix 1*

Preprint of Paper to be submitted for publication in
Nuclear Fusion

Resolving Apparent Differences between Heat and Density Pulse Propagation in JET and TEXT

A.C.C. Sips, G.M.D. Hogeweij[1], A.E. Costley, and J. O'Rourke

JET Joint Undertaking, Abingdon, United Kingdom.

[1]: On attachment from the FOM–Instituut voor Plasmafysica 'Rijnhuizen'. Nieuwegein, Netherlands

N.J. Lopes Cardozo and J.C.M. de Haas[2]

FOM–Instituut voor Plasmafysica 'Rijnhuizen'. Nieuwegein, Netherlands

[2]: Present address: General Atomics, San Diego, California; on attachment from Lawrence Livermore National Laboratories.

Abstract

Sawtooth induced heat and density pulse measurements reported in the literature for the JET and TEXT experiments are addressed. Whereas in JET the heat pulse travels ten times faster than the density pulse, in TEXT both pulses travel at the same speed. The measurements are analysed using coupled transport equations for energy and particles. It is shown that the different behaviour of the density pulse in the two experiments can be attributed to differences in the off–diagonal elements of the transport matrix. If the perturbed fluxes of heat and particles are expressed as linear combinations of the thermodynamic forces ∇p and ∇T (rather than ∇n and ∇T), the corresponding transport matrices are remarkably similar. However, minor differences in this transport matrix between TEXT and JET account for the qualitative difference in the density pulses.

Introduction

Perturbative experiments have become a widely used technique in the study of the transport properties of tokamak plasmas [1]. There are two important differences between steady state transport analysis and perturbative transport experiments. Firstly, in the latter case the incremental diffusivities are evaluated, which may differ substantially from those found by the analysis of steady state profiles. Secondly, perturbative experiments allow an assessment of the possible coupling between heat and particle transport. Experimental data pertinent to the study of coupled transport have been obtained in JET and TEXT, by simultaneous measurements of sawtooth induced heat and density pulses.

The measurements in JET have been analysed using coupled equations for heat and particle transport [2,3]. It was shown that non–zero off–diagonal terms in the transport matrix are required to describe the data. The heat pulse in JET is an order of magnitude faster than the density pulse, yielding a large value of the ratio $(\chi/D)^{inc}$. However, in TEXT the heat and density pulses propagate at the same speed through the confinement region. It is claimed that this is evidence for coupling of heat and particle transport [4–6], but no data analysis which takes coupling into account has been reported.

In this Letter we first present an analysis of the TEXT data in terms of coupled transport, using the analysis techniques developed at JET. Then we compare the TEXT and JET results, and show that no fundamental differences exists between the two experiments.

Summary of experimental results

In TEXT the density pulse is measured using a high–resolution multichannel interferometer system and the heat pulse is measured with a soft X–ray detector array. The density and temperature perturbations are observed to be transported out through the confinement zone at the same rate with nearly identical pulse shapes [4–6]. The initial perturbation of the electron temperature is typically 3 times larger than the perturbation of the density profile. It is reported however, that in low q_a discharges in TEXT and in plasmas near the density limit the heat and density pulses are not identical [4]. In this case the perturbation of the electron density is 1 to 2 times smaller than the temperature perturbation. Analysing the data without accounting for coupling, typical values of χ^{inc} and D^{inc} are found in the range 2 to 6 m^2/s exceeding the values obtained from power balance analysis by a factor 2 to 5. The value of D^{inc} deduced from density pulse propagation is $2-5$ times larger than the value of D^{inc} from oscillating gas puff experiments and ECRH power modulation experiments in TEXT, which is typically 1 m^2/s [7].

Coupled Transport

Since the scale–length of the perturbations is small compared to the gradient lengths of the steady state profiles, the highest order spatial derivatives dominate the transport equations. As a result the propagation of heat and density pulses can be described by a set of two diffusion equations [2,8,9]:

$$\frac{\partial \mathbf{z}}{\partial t} = \mathbf{A}\, \nabla^2 \mathbf{z} \tag{1}$$

with

$$\mathbf{z} = \begin{bmatrix} n_1/n_0 \\ T_1/T_0 \end{bmatrix} ,$$

where n_1 and T_1 are the perturbations of the equilibrium values n_0 and T_0 respectively. The representation of the particle flux ($-\Gamma = D\nabla n$) and heat flux ($-q = n\chi\nabla T$) is general since we allow the diffusion coefficients χ and D to be functions of the local plasma parameters. As a result only dependences on ∇n and ∇T appear in the linearised transport matrix;

$$\mathbf{A} = \begin{bmatrix} D^{inc} & \dfrac{\partial D}{\partial \nabla \mathbf{T}} \dfrac{T_0}{n_0} \nabla \mathbf{n}_0 \\ \\ \dfrac{2}{3} D^{inc} + \dfrac{2}{3} \dfrac{\partial \chi}{\partial \nabla \mathbf{n}} \dfrac{n_0}{T_0} \nabla \mathbf{T}_0 & \dfrac{2}{3} \chi^{inc} + \dfrac{2}{3} \dfrac{\partial D}{\partial \nabla \mathbf{T}} \dfrac{T_0}{n_0} \nabla \mathbf{n}_0 \end{bmatrix} \tag{2}$$

defining

$$D^{inc} \equiv D + \frac{\partial D}{\partial \nabla n} \nabla n_0 \qquad \chi^{inc} \equiv \chi + \frac{\partial \chi}{\partial \nabla T} \nabla T_0 \qquad (3)$$

The spatial distributions of the initial perturbations of the electron density and temperature, induced by the sawtooth are to good approximation identical. Hence, the ratio $\alpha = (n_1/n_0)/(T_1/T_0)$ is independent of the minor radius, and the initial perturbations can be represented by a vector in the $n_1/n_0 - T_1/T_0$ plane (see Fig.1). The eigenvectors of the matrix **A** are also shown in Fig 1a. If the initial perturbation vector coincides with one of the eigenvectors, the relaxation is an eigenmode of the coupled equations. The evolution of the temperature and density profiles is described by a single diffusion coefficient, and the heat and density pulses travel at the same speed and have identical shapes. In general however, a sawtooth collapse excites a combination of the two eigenmodes (see Fig.1a).

Analysis of TEXT heat and density pulses

The heat and density pulses at TEXT are transported out through the confinement zone at the same rate and have identical shape at every radial position:

$$n_1/n_0\,(t) = \alpha\, T_1/T_0\,(t)$$

In terms of eigenmode analysis corresponds to the launching of a single eigenmode of the coupled transport equations (see Fig.1b). Inserting this into the set of coupled equations (1), the following relation between the transport coefficients can be derived

$$A_{22} - A_{11} = A_{12}/\alpha - \alpha\, A_{21} \qquad (4)$$

where the value of α at TEXT is normally quoted as 0.3 [4]. From this equation no unique solution for the matrix elements can be found.

The TEXT data are also simulated with the analysis code developed at JET [3]. The off–diagonal term A_{21} is difficult to determine from pulse measurements [3] and in the calculations A_{21} is assumed to be $2A_{11}/3$; this represents the direct coupling due to the energy carried by a particle flux. The off–diagonal term A_{12} is determined by a least squares fit of simulated pulses to the data, for fixed A_{22} (2 m^2/s) and for the ratio A_{22}/A_{11} ranging from 1 to 10. The results thus obtained are in good agreement with the analytic expression eq (4) and are shown in Fig 2. The figure clearly demonstrates that for $A_{22}/A_{11} \approx 1$ ($\chi^{inc} \approx D^{inc}$) the value of A_{12} changes very significantly by variation of either A_{22} or A_{11}. This seems incompatible with the observation that the identical behaviour of the heat and density pulses is maintained in a wide range of plasma conditions.

The off-diagonal term A_{12} is stable for variations in the diagonal terms for $A_{22} > 2A_{11}$ ($\chi^{inc} > D^{inc}$) and a satisfactory description of the TEXT data is obtained. An important aspect is that in this case the density pulse is governed by the fast eigenvalue, which is substantially higher than the slow eigenvalue. This could lead to an incorrect interpretation of the data if coupling is not taken into account. In other perturbative experiments (i.e. gas puffing) in TEXT [7] where different, or no, temperature perturbations are generated, the evolution of the density is determined by D^{inc}. In particular, for a larger value of α both eigenmodes will be launched. This may explain the divergence of the heat and density pulses which is observed in low q_a and high density discharges, where α is increased to a value larger than 0.5 [4]. In this interpretation, no estimates of the absolute value of A_{11} and A_{21} can be obtained from the TEXT heat and density pulse data.

In summary the application of coupled transport analysis to the TEXT data offers an explanation for a number of observations: the identical pulse shapes are a necessary consequence of an eigenmode, launched by the sawtooth. Second, the discrepancy between the diffusivity derived from the sawtooth induced density pulse propagation and oscillating gas puff experiments arises from the fact that the sawtooth driven density pulse is governed by the large eigenvalue of **A** , whereas the density pulses driven by oscillating gas puff and other perturbative experiments yield a value corresponding to the smaller eigenvalue ($\approx D^{inc}$). Finally, the observed divergence of the heat and density pulses in low q_a and high density discharges occurs since both the slow and the fast eigenmode are launched. This is due to the fact that in these regimes the ratio $(n_1/n_0)/(T_1/T_0)$ is increased by a factor two [4].

Comparison of TEXT and JET results, and Discussion

The effect of coupling from heat and density pulse measurements in JET is observed as an initial decrease of the local density at the time the temperature perturbation reaches its maximum [3]. A comprehensive numerical analysis of the data, including possible perturbed sources and damping, confirmed the results of a description of the pulses using eigenmode analysis [2].

From the heat and density pulse measurements in TEXT, only a limited amount of information about matrix **A** can be extracted. In particular, the value of A_{11} can not be obtained from density pulse measurements. To give a full evaluation of **A**, we shall use the value of A_{11} obtained from oscillating gas puff experiments, i.e. $A_{11} \approx 0.8$ m²/s in the saturated density regime in TEXT [7]. This is justified within the framework of the analysis, where any perturbation of the electron density should evolve with D^{inc} (A_{11}), in the absence of any temperature perturbation. With $A_{22} = 2$ m²/s and A_{21} taken to be $2A_{11}/3$, eq. 4 can be solved for A_{12}, and since $A_{22}/A_{11} > 2$ this solution is numerically stable. Thus, representative TEXT and JET [3] transport matrices are:

$$A_{TEXT} = \begin{bmatrix} 0.8 & 0.3 \\ 0.5 & 2.0 \end{bmatrix} \qquad A_{JET} = \begin{bmatrix} 0.3 & -0.5 \\ 0.2 & 2.0 \end{bmatrix}$$

A_{11} is larger in TEXT than in JET. This difference may be attributed, at least in part, to the fact that the TEXT discharges are hydrogen plasmas, whereas in JET deuterium is used. This isotope effect has already been reported in the literature [10]. A_{22} is similar in both experiments. The most striking difference in the transport matrices is that A_{12} is positive in TEXT and negative in JET. This difference can be observed directly in the density pulse data for both experiment; $A_{12} \approx 0.3$ in TEXT gives a density pulse which is equal to the heat pulse, whereas in JET $A_{12} < 0$ causes a small negative perturbation before the main positive density pulse [3].

In order to interpret this difference in sign of the off–diagonal term it is useful to express the particle and heat fluxes as linear combinations of the gradients. From thermodynamic arguments it can be shown that the relevant thermodynamic forces are ∇p and ∇T [11], which leads to:

$$
\begin{aligned}
-\Gamma &= -\Gamma_{\text{offset}} + M_{11}\frac{1}{T_0}\nabla p + M_{12}\frac{n_0}{T_0}\nabla T \\
-q &= -q_{\text{offset}} + M_{21}\nabla p + M_{22}\, n_0 \nabla T
\end{aligned}
\tag{5}
$$

Insofar as ∇p and ∇T are the forces driving the transport, the matrix **M** is considered to represent the fundamental transport coefficients and can be derived from matrix **A**, yielding:

$$
M = \begin{bmatrix} A_{11} & A_{12} - A_{11} \\ 3A_{21}/2 - A_{11} & 3(A_{22}-A_{21})/2 + A_{11} - A_{12} \end{bmatrix} \tag{6}
$$

$$
\mathbf{M}_{\text{TEXT}} = \begin{bmatrix} 0.8 & -0.5 \\ 0 & 2.8 \end{bmatrix} \qquad \mathbf{M}_{\text{JET}} = \begin{bmatrix} 0.3 & -0.8 \\ 0 & 3.5 \end{bmatrix}
$$

In this interpretation, the underlying transport as described by matrix **M** is essentially the same in both experiments. The main difference is brought about by the value of $D^{\text{inc}} = A_{11} = M_{11}$, which is larger in TEXT than in JET. This difference in M_{11} results in the different signs of A_{12} in both experiments. A_{12} describes the net particle flux driven by temperature gradients, and results from two competing effects: a pressure–gradient–driven diffusive flux, which transports particles down the temperature gradient ($M_{11} > 0$), and a temperature gradient driven flux, which transports particles up the temperature gradient ($M_{12} < 0$). As a result of the difference in the sign of A_{12}, the eigenvectors of **A** in TEXT have a different orientation in the $n_1/n_0 - T_1/T_0$ plane than in JET (see Fig 1). Because the fast eigenvector in TEXT lies close to the initial perturbation vector, the sawtooth collapse excites a fast eigenmode of the coupled diffusion equations. We remark that the comparison is made for typical heat and density pulses in TEXT and JET, a more detailed study is required to confirm our interpretation.

It has been proposed by Hossain [12] and Bishop & Connor [9] that the difference between the values of the transport coefficients obtained from steady state analysis and pulse analysis could result from the presence of non–zero off–diagonal terms in the transport matrix. However, it has been shown in JET [2,3] that the off–diagonal terms give only a small correction, up to 30%, to the values of D^{inc} and χ^{inc} obtained from an analysis which does not take coupling into account. It is stressed that only the functional dependences of χ and D on ∇n and ∇T can give rise to incremental transport coefficients which differ significantly from the steady state values. Finally, it should be realized that the ratio $(\chi/D)^{inc}$ cannot be used as a measure for the steady state value of χ/D.

Conclusions

The observation in TEXT that the heat and density pulses travel through the confinement region at the same speed can be explained by the fact that the sawtooth collapse launches a single eigenmode of the coupled transport equations; the temperature and density pulses travel at the same velocity since both are determined by a single eigenvalue. In contrast a sawtooth collapse in JET usually launches two eigenmodes and thus temperature and density pulses are observed to travel at different velocities. Analysis of heat and density pulses in TEXT shows, that if the result is compared to previously reported results from JET, the underlying transport coefficients are very similar, expressing the particle and heat fluxes as linear combinations of the thermodynamic forces ∇p and ∇T. The main difference seems to be that D^{inc} in TEXT is larger by a factor 2 than D^{inc} in JET. This may be expected from the different discharge conditions in the tokamaks.

Acknowledgements

The authors are indebted to many people at JET, in particular the members of the Electron Temperature Group for stimulating discussions on the subject, and Dr. Schüller, Dr. Stott and Dr. Keilhacker for their constructive comments on the manuscript. The authors are also grateful for the discussions with Dr. Gentle and Dr. Brower from TEXT. Part of this work was performed under the EURATOM–FOM association agreement with financial support from NWO and EURATOM.

References

[1] Lopes Cardozo N.J., de Haas J.C.M., Hogeweij G.M.D., O'Rourke J., Sips A.C.C. and Tubbing B.J.D., inv lecture at 17th Europ. Conf. on Controlled Fusion and Plasma Heating, Amsterdam, (1990), to be published in Plasma Physics and Controlled Fusion.

[2] de Haas J.C.M., O'Rourke J., Sips A.C.C. and Lopes Cardozo N.J., Interpretation of Heat and Density Pulse Measurements in JET in terms of Coupled Transport, Submitted to Nucl Fusion

[3] Hogeweij G.M.D.,O'Rourke J., Sips A.C.C. and de Haas J.C.M., Proc. 17th Europ. Conf. on Controlled Fusion and Plasma Heating, Amsterdam, (1990), Part I 158

[4] Kim S.K., Brower D.L., Foster M.S., McCool S.C., Peebles W.A., Luhmann Jr N.C., Proc. 15th Europ. Conf. on Controlled Fusion and Plasma Heating, Dubrovnik, (1988), Part I 187

[5] Kim S.K. et al, 12th International Conference on Plasma Physics Controlled Nuclear Fusion Research, Nice, (1988), IAEA–CN–50/A–V–2–2.

[6] Brower D.L. et al., Phys. Rev. Lett., **65**, (1990) 337

[7] Gentle K.W., et al, Proc. 17th Europ. Conf. on Controlled Fusion and Plasma Heating, Amsterdam, (1990), Part I 174

[8] Gentle, K., Phys. Fluids, **31**, (1988) 1105

[9] Bishop C.M., Connor J.W., Plasma Phys. Controlled Fusion, **32**, (1990) 203

[10] Gentle, K., Plasma Physics and Contr. Fusion **29**, 9 (1987) 1072

[11] O'Rourke, J., Nucl. Fusion **27** (1987) 2075

[12] Hossain M. et al.,Phys Rev Lett **58** (1987) 487

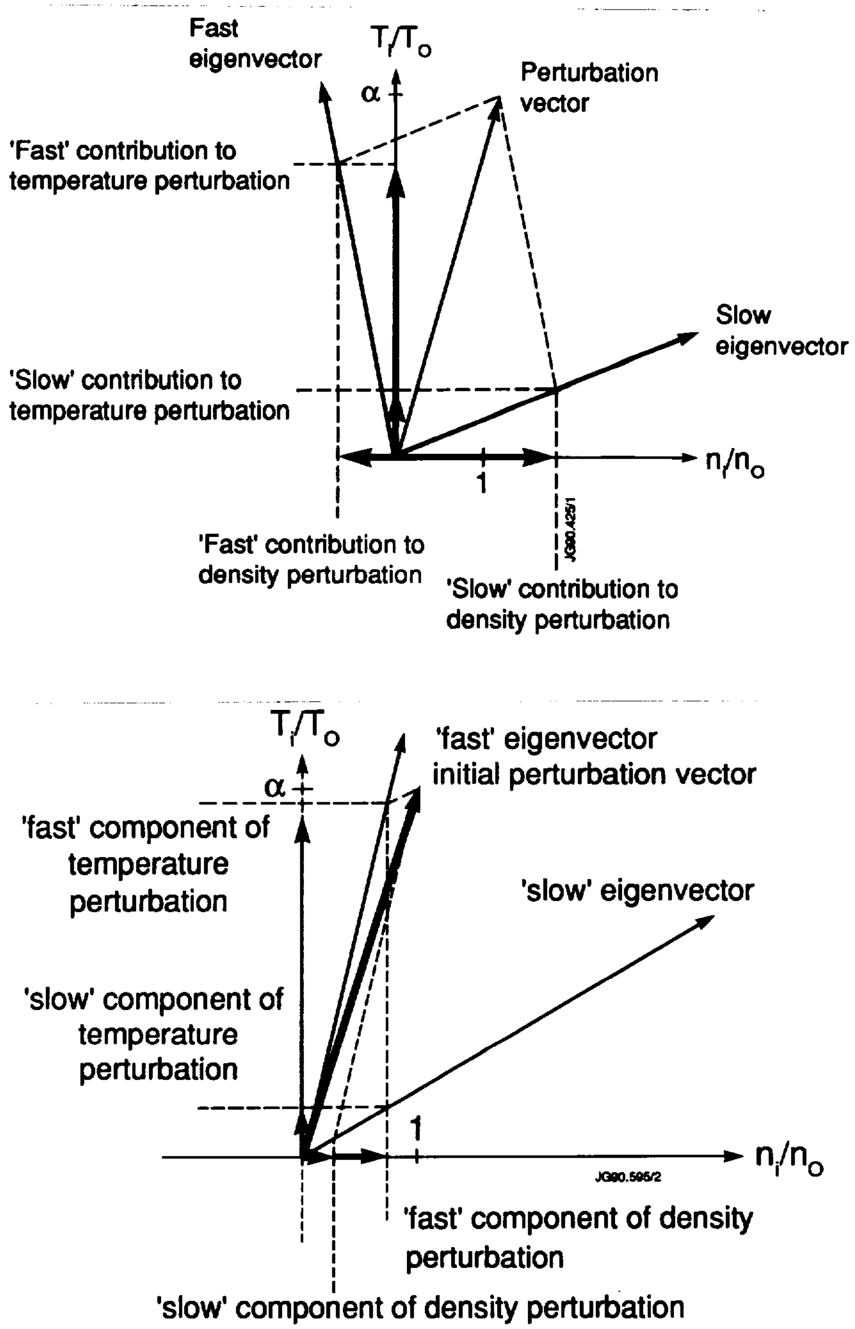

Figure 1.

The initial perturbation of density and temperature can be represented by a vector in the n_1/n_0 – T_1/T_0 *plane and decomposed into eigenvectors of the linearised transport matrix.*

1a; In JET the eigenvalues differ by an order of magnitude so that one can speak of a 'fast' and a 'slow' eigenmode. The eigenvectors are such that the sawtooth launches both fast and slow eigenmodes. The contribution of the fast eigenmode to the density perturbation is negative.

1b; In TEXT a single eigenmode appears to be launched which indicates that the initial perturbation is close to an eigenvector of the transport matrix. The contribution of the fast eigenmode to the density perturbation is positive.

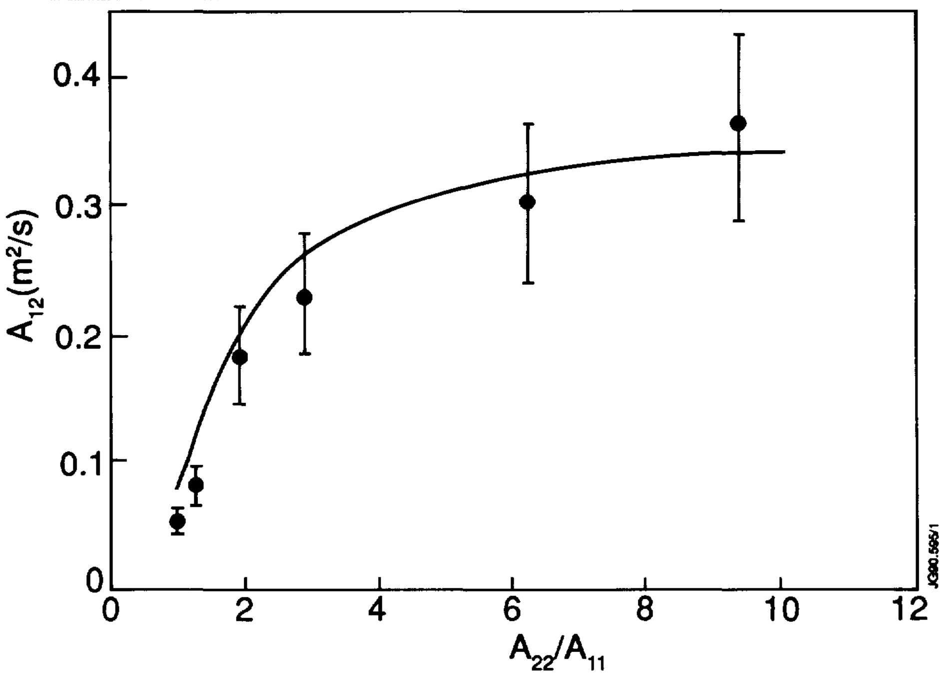

Figure 2.
The value of A_{12} required to describe the TEXT data has been determined for values of A_{22}/A_{11} ranging from 1 to 10. The solid curve represents the analytic expression eq.(4). The points have been obtained by numerical simulation of the data. The error bars indicate the sensitivity of the least square fit to variations in A_{12}.

APPENDIX 1.

THE JET TEAM

JET Joint Undertaking, Abingdon, Oxon, OX14 3EA, U.K.

J.M.Adams[1], F.Alladio[4], H.Altmann, R.J.Anderson, G.Appruzzese, W.Bailey, B.Balet, D.V.Bartlett, L.R.Baylor[24], K.Behringer, A.C.Bell, P.Bertoldi, E.Bertolini, V.Bhatnagar, R.J.Bickerton, A.Boileau[3], T.Bonicelli, S.J.Booth, G.Bosia, M.Botman, D.Boyd[31], H.Brelen, H.Brinkschulte, M.Brusati, T.Budd, M.Bures, T.Businaro[4], H.Buttgereit, D.Cacaut, C.Caldwell-Nichols, D.J.Campbell, P.Card, J.Carwardine, G.Celentano, P.Chabert[27], C.D.Challis, A.Cheetham, J.Christiansen, C.Christodoulopoulos, P.Chuilon, R.Claesen, S.Clement[30], J.P.Coad, P.Colestock[6], S.Conroy[13], M.Cooke, S.Cooper, J.G.Cordey, W.Core, S.Corti, A.E.Costley, G.Cottrell, M.Cox[7], P.Cripwell[13], F.Crisanti[4], D.Cross, H.de Blank[16], J.de Haas[16], L.de Kock, E.Deksnis, G.B.Denne, G.Deschamps, G.Devillars, K.J.Dietz, J.Dobbing, S.E.Dorling, P.G.Doyle, D.F.Düchs, H.Duquenoy, A.Edwards, J.Ehrenberg[14], T.Elevant[12], W.Engelhardt, S.K.Erents[7], L.G.Eriksonn[5], M.Evrard[2], H.Falter, D.Flory, M.Forrest[7], C.Froger, K.Fullard, M.Gadeberg[11], A.Galetsas, R.Galvao[8], A.Gibson, R.D.Gill, A.Gondhalekar, C.Gordon, G.Gorini, C.Gormezano, N.A.Gottardi, C.Gowers, B.J.Green, F.S.Griph, M.Gryzinski[26], R.Haange, G.Hammett[6], W.Han[9], C.J.Hancock, P.J.Harbour, N.C.Hawkes[7], P.Haynes[7], T.Hellsten, J.L.Hemmerich, R.Hemsworth, R.F.Herzog, K.Hirsch[14], J.Hoekzema, W.A.Houlberg[24], J.How, M.Huart, A.Hubbard, T.P.Hughes[32], M.Hugon, M.Huguet, J.Jacquinot, O.N.Jarvis, T.C.Jernigan[24], E.Joffrin, E.M.Jones, L.P.D.F.Jones, T.T.C.Jones, J.Källne, A.Kaye, B.E.Keen, M.Keilhacker, G.J.Kelly, A.Khare[15], S.Knowlton, A.Konstantellos, M.Kovanen[21], P.Kupschus, P.Lallia, J.R.Last, L.Lauro-Taroni, M.Laux[33], K.Lawson[7], E.Lazzaro, M.Lennholm, X.Litaudon, P.Lomas, M.Lorentz-Gottardi[2], C.Lowry, G.Magyar, D.Maisonnier, M.Malacarne, V.Marchese, P.Massmann, L.McCarthy[28], G.McCracken[7], P.Mendonca, P.Meriguet, P.Micozzi[4], S.F.Mills, P.Millward, S.L.Milora[24], A.Moissonnier, P.L.Mondino, D.Moreau[17], P.Morgan, H.Morsi[14], G.Murphy, M.F.Nave, M.Newman, L.Nickesson, P.Nielsen, P.Noll, W.Obert, D.O'Brien, J.O'Rourke, M.G.Pacco-Düchs, M.Pain, S.Papastergiou, D.Pasini[20], M.Paume[27], N.Peacock[7], D.Pearson[13], F.Pegoraro, M.Pick, S.Pitcher[7], J.Plancoulaine, J-P.Poffé, F.Porcelli, R.Prentice, T.Raimondi, J.Ramette[17], J.M.Rax[27], C.Raymond, P-H.Rebut, J.Removille, F.Rimini, D.Robinson[7], A.Rolfe, R.T.Ross, L.Rossi, G.Rupprecht[14], R.Rushton, P.Rutter, H.C.Sack, G.Sadler, N.Salmon[13], H.Salzmann[14], A.Santagiustina, D.Schissel[25], P.H.Schild, M.Schmid, G.Schmidt[6], R.L.Shaw, A.Sibley, R.Simonini, J.Sips[16], P.Smeulders, J.Snipes, S.Sommers, L.Sonnerup, K.Sonnenberg, M.Stamp, P.Stangeby[19], D.Start, C.A.Steed, D.Stork, P.E.Stott, T.E.Stringer, D.Stubberfield, T.Sugie[18], D.Summers, H.Summers[20], J.Taboda-Duarte[22], J.Tagle[30], H.Tamnen, A.Tanga, A.Taroni, C.Tebaldi[23], A.Tesini, P.R.Thomas, E.Thompson, K.Thomsen[11], P.Trevalion, M.Tschudin, B.Tubbing, K.Uchino[29], E.Usselmann, H.van der Beken, M.von Hellermann, T.Wade, C.Walker, B.A.Wallander, M.Walravens, K.Walter, D.Ward, M.L.Watkins, J.Wesson, D.H.Wheeler, J.Wilks, U.Willen[12], D.Wilson, T.Winkel, C.Woodward, M.Wykes, I.D.Young, L.Zannelli, M.Zarnstorff[6], D.Zasche[14], J.W.Zwart.

PERMANENT ADDRESS

1. UKAEA, Harwell, Oxon. UK.
2. EUR-EB Association, LPP-ERM/KMS, B-1040 Brussels, Belgium.
3. Institute National des Récherches Scientifique, Quebec, Canada.
4. ENEA-CENTRO Di Frascati, I-00044 Frascati, Roma, Italy.
5. Chalmers University of Technology, Göteborg, Sweden.
6. Princeton Plasma Physics Laboratory, New Jersey, USA.
7. UKAEA Culham Laboratory, Abingdon, Oxon. UK.
8. Plasma Physics Laboratory, Space Research Institute, Sao José dos Campos, Brazil.
9. Institute of Mathematics, University of Oxford, UK.
10. CRPP/EPFL, 21 Avenue des Bains, CH-1007 Lausanne, Switzerland.
11. Risø National Laboratory, DK-4000 Roskilde, Denmark.
12. Swedish Energy Research Commission, S-10072 Stockholm, Sweden.
13. Imperial College of Science and Technology, University of London, UK.
14. Max Planck Institut für Plasmaphysik, D-8046 Garching bei München, FRG.
15. Institute for Plasma Research, Gandhinagar Bhat Gujat, India.
16. FOM Instituut voor Plasmafysica, 3430 Be Nieuwegein, The Netherlands.
17. Commissiariat à L'Energie Atomique, F-92260 Fontenay-aux-Roses, France.
18. JAERI, Tokai Research Establishment, Tokai-Mura, Naka-Gun, Japan.
19. Institute for Aerospace Studies, University of Toronto, Downsview, Ontario, Canada.
20. University of Strathclyde, Glasgow, G4 ONG, U.K.
21. Nuclear Engineering Laboratory, Lapeenranta University, Finland.
22. JNICT, Lisboa, Portugal.
23. Department of Mathematics, Univeristy of Bologna, Italy.
24. Oak Ridge National Laboratory, Oak Ridge, Tenn., USA.
25. G.A. Technologies, San Diego, California, USA.
26. Institute for Nuclear Studies, Swierk, Poland.
27. Commissiariat à l'Energie Atomique, Cadarache, France.
28. School of Physical Sciences, Flinders University of South Australia, South Australia SO42.
29. Kyushi University, Kasagu Fukuoka, Japan.
30. Centro de Investigaciones Energeticas Medioambientales y Techalogicas, Spain.
31. University of Maryland, College Park, Maryland, USA.
32. University of Essex, Colchester, UK.
33. Akademie de Wissenschaften, Berlin, DDR.

CR 88.49.1A